A SQUID magnetometry system for a cryogenic neutron electric dipole moment experiment

S. Henry[1], *C. Clarke, A. Cottle, A. Lynch, M. Pipe.*
University of Oxford, Denys Wilkinson Building, Keble Road, Oxford OX1 3RH, UK.

Abstract

Precision magnetometry is an essential component of any neutron electric dipole moment experiment in order to correct shifts in the neutron precession frequency due to changes in the magnetic field. We have developed a magnetometry system using 12 SQUID sensors, designed to operate in 0.5K superfluid helium. The pick-up loops located near the neutron cell are connected to the SQUID sensors by ~2m twisted wire pairs. The SQUID readout cables are run via an intermediate stage at 4.2K. The system has been installed and tested in the cryoEDM apparatus at the ILL, Grenoble, and used to characterise the magnetic environment. Further tests in a suitable low noise environment confirm it meets our requirements.

Keywords: Neutron EDM; Magnetometer; SQUID

1. Introduction

There are a number of projects around the world aiming to measure the electric dipole moment of the neutron to an improved precision. A non-zero measurement of this quantity would demonstrate the violation of T-symmetry. Precision measurements offer a way to test for new physics beyond the standard model [1].

These experiments search for a shift in the neutron spin precession frequency, when the direction of an applied electric field is reversed. It is essential to monitor any change in the magnetic field in the neutron cell between these measurements in order to correct for the resulting frequency shifts. Past neutron EDM experiments have used a range of different magnetometers. The current experimental limit on the neutron EDM ($|d_n|<2.9\times10^{-26}$e·cm) [2] was set using an atomic mercury magnetometer [3,4]. The magnetometry is critical to the performance of the experiment.

Operating at cryogenic temperatures restricts the choice of magnetic sensor. However this is required for experiments such as cryoEDM [5-7], and the SNS neutron EDM experiment [8,9], which operate at 0.5K in order to exploit the higher flux of ultra-cold neutrons which can be produced using a super thermal source [10]. This rules out the use of the mercury magnetometer.

In this paper we describe a SQUID magnetometry system designed to measure the magnetic field in the cryoEDM experiment. The SQUID pick-up loops cannot be positioned very close to the neutron cell, due to the high electric field required for the EDM measurement, therefore we must extrapolate the field from measurements from multiple loops ~0.2m from the neutron cell. A uniform magnetic environment is essential to avoid the systematic error resulting from the geometric phase effect [11], and maintain the polarization of the neutrons (in the neutron guides as well as the storage cell). The design specification for the cryoEDM experiment is a maximum gradient of 0.1nT/m in the storage cell [12].

Therefore the magnetometry must not distort either the field it measures, or that around the neutron guides. As the system is run in superfluid helium at 0.5K, we require a readout system which does not introduce a significant heat load.

[1] Corresponding author: s.henry@physics.ox.ac.uk

In the following sections, we give an overview of magnetometry for neutron EDM measurements; the cryoEDM experiment; the requirements for such a magnetometer; and SQUIDs. In Section 6 we give an overview of the magnetometer, with details of the key components including the pick-up loops, the superconducting capillary shields, the Stycast filled feedthroughs, and the readout cabling, electronics and software. We then report on tests conducted in the low noise Laboratoire Souterrain à Bas Bruit (LSBB) laboratory.

2. Magnetometry for neutron EDM experiments

The neutron Larmor spin precession frequency in a uniform electric field **E** and magnetic field **B** is given by

$$h\nu = \left|2\boldsymbol{\mu}\cdot\mathbf{B} \pm 2\mathbf{d}\cdot\mathbf{E}\right| \quad (1)$$

Where **μ** is the magnetic dipole moment and **d** is the electric dipole moment, and the ± sign represents parallel or antiparallel fields. Neutron EDM experiments search for a non-zero **d,** by looking for a shift in this frequency correlated with a change in the electric field. However as the **μ·B** term is eight orders of magnitude larger than **d·E**, this must be measured to correct for shifts due to magnetic fluctuations. Therefore a neutron EDM experiment requires a precision measurement of shifts in two key quantities: the neutron precession frequency, and the magnetic field.

In the first neutron EDM experiments [13], the magnetic field was monitored using proton magnetometers. A wide range of instruments have been used for different experiments since then, and neutron EDM measurements have provided a motivation for the development of precision magnetometry.

An earlier experiment by the ILL/RAL/Sussex collaboration [14] monitored the magnetic field using three rubidium-vapour magnetometers. As this result was limited by the distance between the neutron cells and the magnetometers, and their internal drifts, the collaboration then developed a cohabiting mercury magnetometer [3] in which the field in the neutron cell is directly measured from the precession frequency of polarized ^{199}Hg nuclei. The instrument made systematic uncertainties due to magnetic field fluctuations negligible. Unfortunately, it is not suitable for cryogenic temperatures.

Our design is unique in the use of SQUIDs to directly monitor the magnetic field changes. The planned neutron EDM experiment at SNS [8,9] are developing a co-magnetometer suitable for cryogenic temperatures using SQUID sensors to measure the magnetic signal from precessing ^{3}He nuclei [15,16]. A ^{3}He magnetometer for neutron EDM measurements has also been developed with a gas sample stored in a separate cell [17]. All other neutron EDM experiments use some form of atomic magnetometry. The PNPI-ILL-PTI collaboration have reported a new neutron EDM limit using a double cell experiment surrounded by eight caesium magnetometers [18].The PSI experiment [19] will use a Hg co-magnetometer [20], supplemented by caesium vapour magnetometers [21,22]. The TUM experiment [23] plan to use ^{199}Hg and other magnetometers. The KEK/TRIUMF experiment [24] are investigating ^{129}Xe [25,26].

3. The cryoEDM experiment

The CryoEDM experiment is based on the same measurement principle as the previous RAL/Sussex experiment at ILL. This measurement used stored polarized ultra-cold neutrons (UCN). The frequency measurement was made using the Ramsey separated oscillatory field magnetic resonance technique [27], in which an oscillating field close to the Larmor frequency is applied to rotate the neutron spins by 90°. There then follows a period of free precession, typically ~130 seconds – limited by the lifetime of the stored neutrons, before a second oscillatory field, in phase with the first, is applied. The number of neutrons in each polarization state is then counted. Any difference between the frequency of the applied field and the spin precession frequency will cause a phase difference to

build up over the storage time. The precession frequency measurement was repeated many times over several months of data taking with periodic reversals of the electric and magnetic field. The EDM measurement was made by measuring the shift in the precession frequency when the electric field was reversed.

With the systematic errors due to magnetic field fluctuations made insignificant by the mercury magnetometer, the experiment, using a UCN source consisting of a liquid-deuterium cold source and a total-reflection neutron turbine [28], was limited by the statistics. It was decided that the best strategy to improve the sensitivity was to move to a cryogenic experiment.

The principle of a superthermal UCN source was first proposed in 1977 [29] and demonstrated shortly after [30]. This method exploits the properties of superfluid helium, specifically the fact that the dispersion curves for neutrons and superfluid helium cross at a momentum corresponding to 8.9Å. This means that a neutron of this energy can transfer all its energy to a phonon in the helium. At temperatures below 0.8K, the reverse process – the up-scattering of UCN by phonons is negligible, so a large UCN population can be produced. The production rate was measured by the collaboration using neutron detectors within the superfluid helium [10] and is the basis of the cryoEDM experiment, proposed in 2003 [12].

As UCN cannot be efficiently extracted from the superfluid helium, the experiment is designed to carry out all neutron measurements in this environment. UCN can be lost by the absorption of phonons, therefore the temperature must be kept below 1K to minimise the phonon population. The UCN are produced, stored, moved between storage volumes, have their polarization manipulated, and are finally detected, all in superfluid helium, below 0.7K. This requirement introduces numerous technical challenges, necessitating significant changes compared to previous neutron EDM experiments. However it also brings additional benefits: liquid helium can support a larger electric field [31]; low temperatures allow the use of superconducting magnetic shields; and the cryogenic environment helps to remove some impurities which could absorb neutrons.

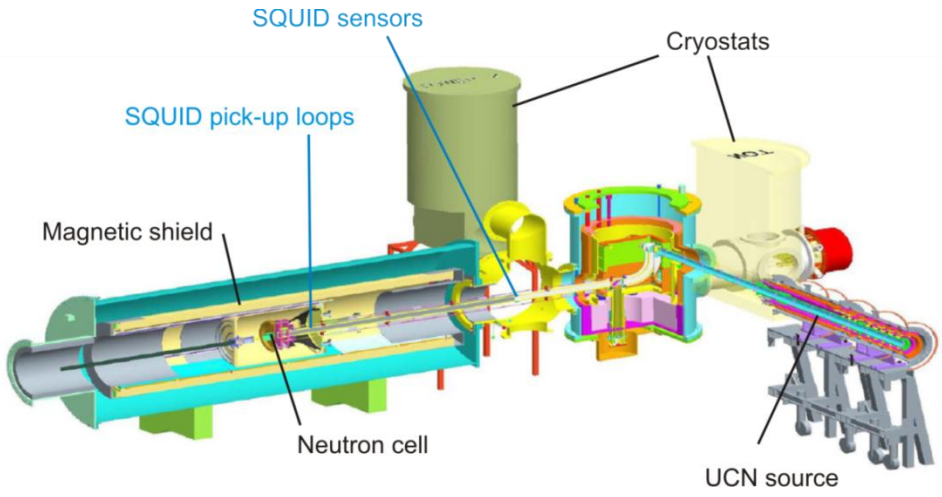

Figure 1 An overview of the cryoEDM apparatus showing the main parts and the location of the main components of the SQUID system. The neutron beam from the ILL reactor enters from the right into the superthermal UCN source. The neutrons are stored for the Larmor frequency measurement in neutron cells at the centre of the superconducting magnetic shield.

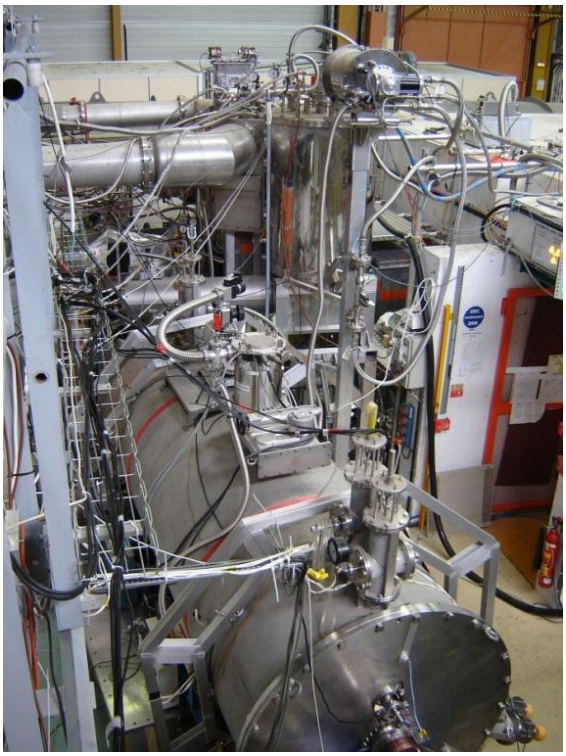

Figure 2 A photograph of the cryoEDM apparatus at ILL. The horizontal cylinder in the foreground is the magnetic shield. Behind this is the UCN source and cryostats to cool the apparatus. The neutron beam enters from the right.

The experiment is located at the Institut Laue-Langevin, Grenoble. An overview is shown in Figure 1 and a photograph in Figure 2. The superfluid volume is cooled by a ^{3}He circulation refrigerator driven by a set of roots pumps. This is surrounded by thermal shields cooled to liquid helium and liquid nitrogen temperatures. The superfluid is passed through a superleak to remove ^{3}He [32], which would give significant neutron losses due to its large absorption cross section.

The 9Å polarised neutron beam is delivered from the ILL reactor via a polariser and monochromator. The UCN are produced by down scattering in superfluid helium inside the source. They then move along neutron guides, made from beryllium coated copper, to the storage cells at the centre of the magnetic shield. A series of valves driven by actuator rods, connected to stepper motors outside the vacuum chamber, are used to control the flow of UCN between the source, the transfer tube, the two neutron cells, and the detectors.

The resonance measurement will be done in two 2.2l cells. One cell is between two neutral electrodes, while the second is between a neutral and a high voltage electrode, producing the electric field. The UCN are detected by solid state detectors with a ^{6}LiF conversion film, so the neutrons are detected by the n(^{6}Li,^{3}H)^{4}He reaction. These detectors have been shown to work well even within superfluid helium [33,34].

The neutron cells are at the centre of a series of magnetic shields consisting of three layers of mu-metal and a superconducting Pb cylinder. The holding field of 5μT is produced by a superconducting solenoid. The neutron cells are inside a superfluid containment vessel made from low magnetic stainless steel. A set of trim coils are used to adjust the magnetic field to optimise the uniformity.

4. Requirements of the cryoEDM magnetometry system

The location of the cryoEDM experiment in the ILL experimental hall experiences large fluctuations in the magnetic field, generated by other experiments such as the IN15 spin echo spectrometer [35], and activity such as the movement of the overhead crane. The magnitude of these disturbances is substantially attenuated by the mu-metal and superconducting Pb shielding around the apparatus.

The precision magnetometer is required to monitor the residual fluctuations in the magnitude of the magnetic field averaged over the neutron cell, in order to correct the resulting shift in the neutron precession frequency due to the **μ·B** term in equation 1.

The frequency shift corresponding to the current nEDM limit (2.9×10^{-26}e·cm) is equivalent to a magnetic field change of 4.3fT in that experiment. This represents the difference between the magnetic field averaged over all runs with parallel, and that over all runs with an antiparticle electric field. (A neutron EDM measurement is made by averaging the frequency shift over N~10^4 electric field reversals). The target resolution to which a magnetometer must track the change in magnetic field across a single electric field reversal is not as demanding as the statistics mean

$$\Delta B_{\text{all data}} = \frac{1}{\sqrt{N}} \Delta B_{\text{single measurement}}$$

So the resolution requirement for a magnetometer is

$$\Delta B = \frac{d\Delta E}{\mu} \sqrt{N}$$

To reach an EDM sensitivity of d=10^{-27}e·cm in an experiment with an electric field of ΔE=80kV/cm over N=10,000 runs, this gives a magnetometer resolution of 0.1pT. This was the resolution achieved by the nEDM mercury magnetometer [3] and the target for the cryoEDM system. We quote this as an example of how this sensitivity could be achieved. However it may also be achieved with a smaller number of runs, and a greater magnetometer resolution per run.

We have measured the intrinsic noise of our SQUID sensors, and shown this is equivalent to a magnetometer noise of 2.6 fT·Hz$^{-1/2}$ above 1Hz, and (3.2/√(f/1Hz)) fT·Hz$^{-1/2}$ below this [36]. This is typical for low temperature SQUIDs [37,38]. In most SQUID applications the measured resolution is limited by the external magnetic noise. In the final cryoEDM setup, we aim to reduce this, with magnetic shielding, to a level where we are limited by the intrinsic SQUID noise. The FWHM resolution of a magnetometer over a measurement period T, with a noise level of $B_n(f)$, at frequency f is given by:

$$\delta B = 2.35 \sqrt{\int_{\frac{1}{T}}^{f_{max}} B_n^2(f) df}$$

For the noise level quoted above, with a T=1,000s measurement time and 1Hz cut-off (required for cryoEDM measurements) this gives a resolution of 20fT. Therefore in principle, SQUID sensors can exceed the required performance. The challenge is to build a system which is limited by the intrinsic SQUID noise and not by external magnetic noise or other effects.

To correct neutron frequency shifts, we need to determine the magnetic field magnitude averaged over the neutron storage volume. In the previous experiment, this was measured directly using the ^{199}Hg co-magnetometer. However SQUIDs, like most magnetic field sensors cannot be placed in the neutron volume, as they would be damaged by the high electric field, and interfere with the neutron measurement. We therefore require a multi-channel system to allow the extrapolation of the field in a remote volume from measurements made with SQUIDs at multiple points away from this.

The cryoEDM experiment will take a simultaneous measurement of the neutron precession frequency in two cells: a HV cell in an electric field, and a control neutral cell. The neutral cell neutron measurement will, in effect, be used as a magnetometer, and will be used to calibrate the SQUID system. The SQUIDs will then provide a faster, more direct way to monitor the magnetic field; and will be used to determine the gradient of the field fluctuations between the two cells, and provide an independent measurement. Thus we will control this significant systematic uncertainty.

5. SQUID magnetometry

SQUIDs (Superconducting Quantum Interference Devices) are sensitive instruments which exploit the phenomena of flux quantization and Josephson tunnelling to achieve a sensitivity to changes in the magnetic field at the femtotesla level [37,38]. They have found application as precision magnetometers in fundamental particle physics research in experiments searching for magnetic monopoles [39-41], and also as detector readout for superconducting TES sensors in dark matter experiments [42,43], and microwave detectors in axion searches [44].

SQUIDs can monitor changes in the magnetic field at the fT/√Hz level. However their use in a neutron EDM experiment introduces specific challenges. Unlike atomic magnetometers, they are not sensitive to the absolute value of the magnetic field strength, but only to changes in the magnetic flux through pick-up loops. They have a periodic response to the magnetic flux (with a period of $1\Phi_0$). A feedback loop is used to linearize this response. But if the magnetic field changes faster than the slew rate of the feedback electronics, this can create data artefacts where the signal apparently jumps by a value equivalent to a multiple of $1\Phi_0$. Such 'flux jumps' can also be triggered by electromagnetic interference. We therefore require electromagnetic compatibility measures and control software to deal with this issue.

6. The cryoEDM SQUID magnetometer

Figure 3 shows an overview of the SQUID magnetometry system we have developed and installed in the cryoEDM apparatus. The sensors and pick-up loops are located inside superfluid helium at 0.5K. The pick-up loops are to the side of the neutron cells, at the centre of the main magnetic shield. The SQUID sensors themselves cannot be located in this volume as they would distort the field; therefore the sensors are mounted in a transfer volume just outside the main shield, and are connected to the pick-up loops by long twisted-wire pairs which run through superconducting capillaries.

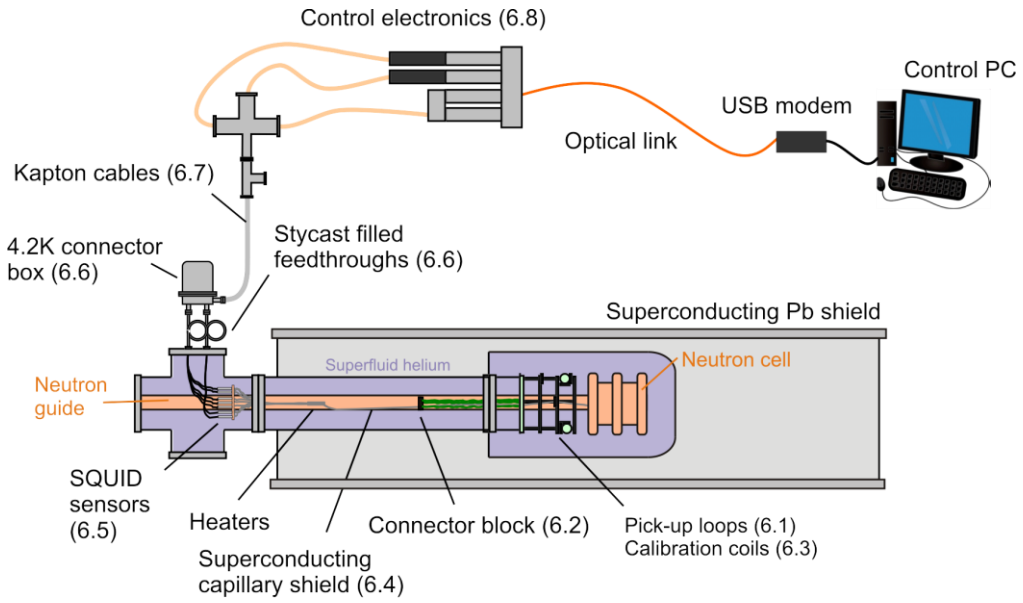

Figure 3 Schematic overview of the cryoEDM SQUID magnetometer. The numbers in parentheses refer to the sub-sections where each component is described.

To minimise the heat load into the superfluid volume, the readout cables for the SQUIDs are split into two sections, joined by a heat sink and connector box at 4.2K. The connection from here into the superfluid is through superconducting NbTi twisted wire pairs. The cables which carry the signals

to the connector box on the top of the cryostat are flat Kapton ribbon cables with stainless steel tracks.

6.1. Pick-up loops

The pick-up loops are made from NbTi wire on a support structure built of G10 epoxy. The area of the pick-up loops must be chosen carefully. In a low noise environment, the largest possible loop will give the best signal to noise ratio. But if a too-large loop is used in an environment with large magnetic fluctuations (such that $\delta\Phi_{Noise}$~$1\Phi_0$) this will produce a large number of flux jumps, increasing the risk of errors in the signal processing. In addition larger loops will act as a more efficient antenna to RF radiation, and are thus more susceptible to electromagnetic interference. This interference is above the frequency of interest, but it can be demodulated by the SQUID sensor producing drift, or preventing operation altogether [37].

The system is designed to allow the pick-up loop design to be changed easily to accommodate the needs of each cooldown. During commissioning runs, with a non-optimised magnetic shield, small pick-up loops have been used so the magnetic fluctuations due to laboratory activity do not overload the SQUIDs. Once the full shielding factor is achieved, we will use larger loops to achieve a better signal-to-noise ratio. And when the sources of magnetic disturbances have been fully characterised we may change the loop configuration to allow the most effective extrapolation of the magnetic field in the neutron cell from the SQUID data.

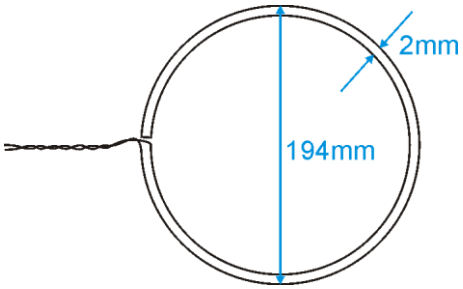

Figure 4 Annular shape used to fit a pick-up loop around the neutron guide, which is symmetric about the axis.

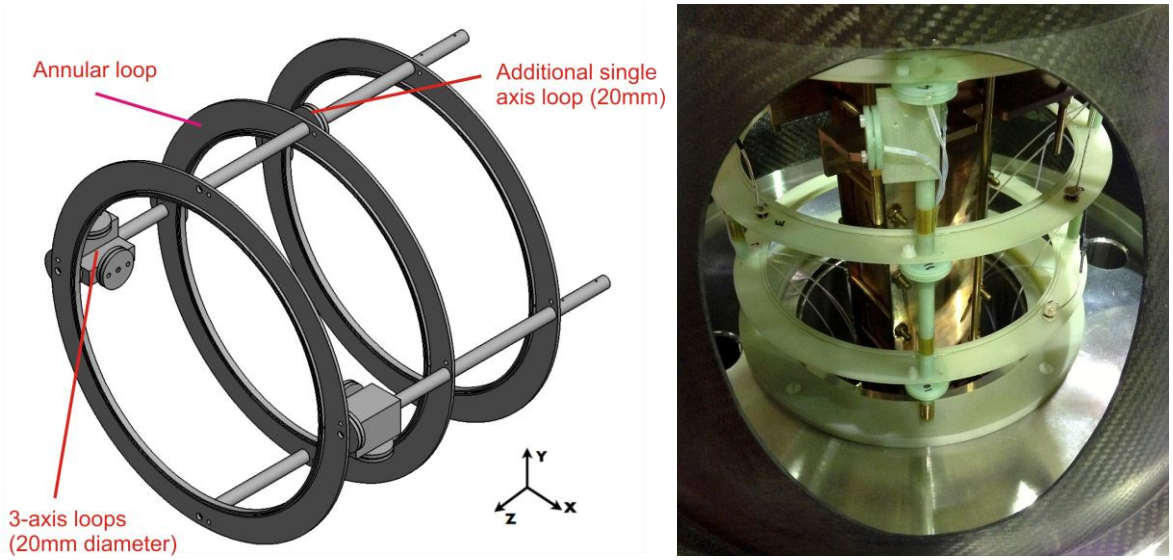

Figure 5 The arrangement of pick-up loops installed during a test run. This includes two 3-axis assemblies of small (20mm) loops; and three small loops, and three larger, annular shaped loops to measure the axial Z component. The outer diameter of the G10 former is 200mm.

The magnetic field generated by the solenoid is oriented along the Z-axis, therefore magnetic field fluctuations in this direction will have then largest impact on the magnitude of the field. Therefore the majority of loops are in this orientation. A small on-axis loop could not fit around the neutron guide, therefore we produced loops of an annular shape shown in Figure 4. This setup allows the measurement of the Z component of the field symmetrically around the axis. A single loop of this diameter would overload the SQUID. The G10 former is designed to align the inner and outer circular loops precisely to minimise transverse pick-up.[2]

Figure 5 shows a typical arrangement of loops used for recent tests with two 3-axis sets of 20mm diameter loops; three additional 20mm loops arranged off-axis in the Z direction; and three annular shaped loops consisting of two wire loops of diameter 190 and 194mm.

6.2. Superconducting connector block

The leads of 0.127mm diameter wire from the pick-up loops are twisted together and run ~1m from the loops, along the neutron guides, to a connector block located outside the main superfluid containment vessel (SCV). At this point they are connected to the shielded twisted wire pairs (TWPs) leading to the SQUID sensors. The connections must be superconducting as even a micro-ohm contact resistance will prevent the system from tracking magnetic fields. The connection block design is show in Figure 6. The wire ends are clamped together inside a short cylinder of solder-wire to form a reliable superconducting contact.

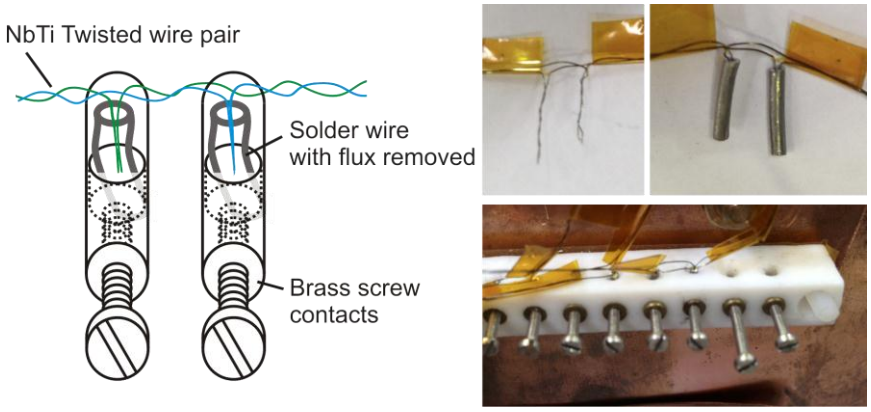

Figure 6 Detail of the connector block used to join the twisted wire pairs from the SQUID sensors, with those from the pick-up loops. The contact must form a superconducting contact. This is done by clamping the two NbTi wires inside a short length of solder capillary. The two wires are drawn in different colours and separated for clarity. In reality they are tightly twisted and arranged so there is no significant loop area which would lead to magnetic pick-up.

Once we had developed the technique for forming contacts, we ran a series of tests with the inputs of a series of SQUIDs connected to a connector block. The superconductivity of the contacts was tested by the method described in [45]. We tested a total of 18 contacts, of which only one was not superconducting on the first test.

[2] We investigated using tinned copper tracks on a fibre glass board as a way to manufacture loops, however it was decided the risk of a large loop of this design not becoming superconducting was too large, therefore conventional NbTi wire loops were used for the final design.

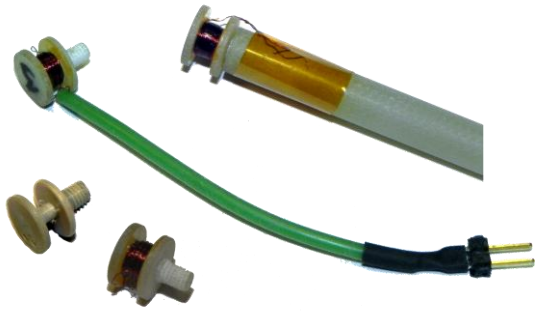

Figure 7 The small coils used to generate a calibration signal. The photo shows the former, wound coils, and support rod and connection lead.

6.3. Calibration coils

The absolute calibration of the SQUID magnetometer will be done from the precession frequency of the neutrons measured with zero applied electric field. However, as the precession frequency measurement takes time, and requires an approximate knowledge of the magnetic field in order to set the signal generator frequency, an independent calibration system is installed using small coils.

Up to twelve calibration coils are mounted on the pick-up loop support shown in Figure 5. These each have ~200 turns wound on a 1mm diameter former as pictured in Figure 7. The connection is made using long copper twisted-wire-pairs, which run along the neutron guide and connect to the Stycast feedthroughs described in Section 6.6. The signal seen by each SQUID channel for each calibration coil is calculated by numerically integrating the field across the area of each pick-up loop. The coils can be accurately modelled as a magnetic dipole at distances of more than ~50mm from the coils.

6.4. Superconducting capillaries

The superconducting twisted wire pairs that join the pick-up loops to the SQUID sensors pass outside of the main magnetic shielding. Without additional magnetic shielding, they would pick-up magnetic field fluctuations within this region. Therefore the wires must be clad with an additional superconducting magnetic shield. These magnetic shields consist of Pb-Sn solder wire in which the flux core has been removed, creating a capillary, through which the TWPs are run. The production and characterisation of these capillaries is described in detail in [46]. Here we give a short summary of our design.

The TWP shields are made in two sections. The wires from the SQUID sensors pass through thin capillaries made from single-core solder for ~0.3m; then three of these are joined to a 1.2m capillary made from triple-core solder, where each core provides a path for one TWP. The join between the two sections is shielded by a 5.2mm diameter cylindrical piece machined from Pb. The cylinder contains a heater, made from a 390Ω resistor. This is illustrated in Figure 8. The enclosure is filled with Stycast to ensure the heater is thermally isolated from the superfluid helium. The heater allows the input loop to be heated into its conducting state, to destroy any supercurrent in the loop, while the SQUID sensor remains superconducting so we can monitor this state, which would not be possible using the heater on the SQUID chip.

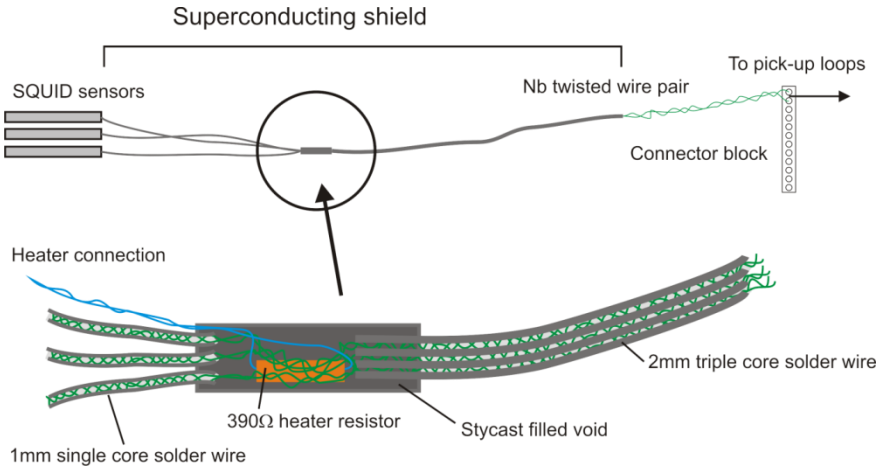

Figure 8 Schematic drawing of the superconducting shield assembly to shield the twisted wire pairs between the SQUID sensors and the pick-up loops

To attenuate any unwanted signals due to magnetic pick-up in the TWPs to the target level of 0.1pT, a magnetic shielding factor of at least 80,000 is required. We have carried out a series of tests to confirm that this requirement is met. Further details are given in [46].

6.5. SQUID sensors

The twelve SQUID sensors were supplied by Supracon AG (model CS Blue). These each had an integrated input coil, feedback coil and heater. The TWP from the pick-up loop was connected to the input coil using small Nb screw terminals. A RC filter across the input reduced the susceptibility to high frequency interference. The input was connected to ground via a 10kΩ resistor to prevent a large voltage of the input damaging the sensors (a significant risk as the pick-up loops are close to high voltage electrodes). The voltage across the SQUID was measured via a cold transformer. Figure 9 shows a photograph of the sensor. The same SQUID package was used for detector readout in the CRESST dark matter search [43]. Table 1 gives the SQUID parameters taken from the Supracon data sheets. The flux noise measured in Oxford with a shunted input was $2.8\mu\Phi_0/Hz^{-1/2}$.

Parameter	**Value**
SQUID inductance	≈400pH
Input inductance	≈350nH
Feedback coupling	$9.1\mu A/\Phi_0$
Input coupling	$0.21\mu A/\Phi_0$
Equivalent flux noise	$6.2\mu\Phi_0/Hz^{1/2}$

Table 1 SQUID parameters (open input, 4.2K)

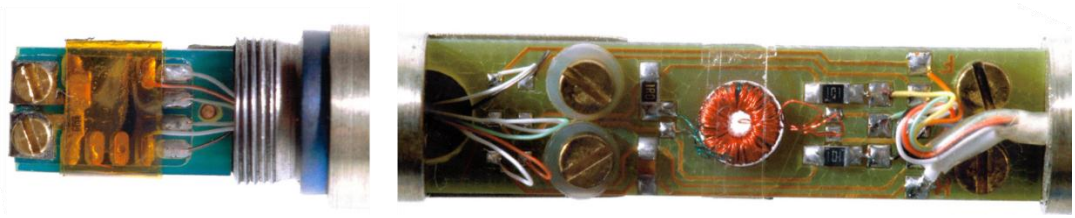

Figure 9 The SQUID chip (left) supplied by Supracon AG, and cold transformer board (right) from STAR Cryoelectronics .

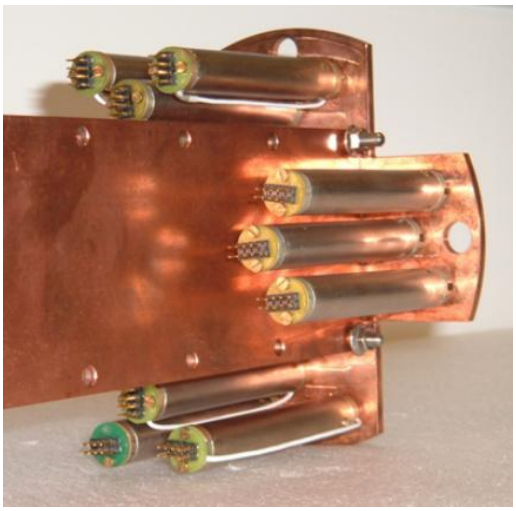

Figure 10 The twelve SQUID sensors with individual Cryoperm shields, mounted onto the neutron guide.

The SQUID chip was shielded from magnetic fluctuations by a 22mm length Nb cylinder. This (and the cold transformer board) was mounted inside a high permeability Cryoperm cylinder. The Cryoperm shield significantly reduces the magnetic flux frozen in the superconducting Nb shield, the body of the SQUID and the superconducting input circuit, which could lead to higher 1/f noise due to the motion of trapped vortices [37]. This is a significant problem for high-T_c SQUIDs. It is unclear if it is so important at the 0.5K temperatures where we operate. However as excess 1/f noise could critically impair the performance of the system, it was decided it was too risky to operate without the cryoperm.

The twelve SQUID sensors were mounted around the neutron guide as shown in Figure 10. The presence of the Cryoperm shields creates a local distortion in the static magnetic field. Simulations showed there was a risk this could cause a significant depolarisation of the neutrons in this volume. Therefore a customised solenoid was installed around the neutron guide at this point to compensate for this field distortion. Simulations of the magnetic field were done using the OPERA finite element analysis software.

6.6. Stycast filled feedthroughs and connector box: 4.2 – 0.5K

The readout connections from the SQUID sensors to the top of the cryostat were made in two stages. The SQUID sensors are connected to a set of NbTi twisted wire pairs, which run upwards through spiral stainless-steel tubes, filled with Stycast epoxy. These connect to heat sinks thermally anchored to 4.2K, inside a connector box, from where Kapton cables run to the top of the cryostat. This setup, illustrated in Figure 11, was designed to minimise the heat load onto the superfluid, while providing a low electrical impedance readout.

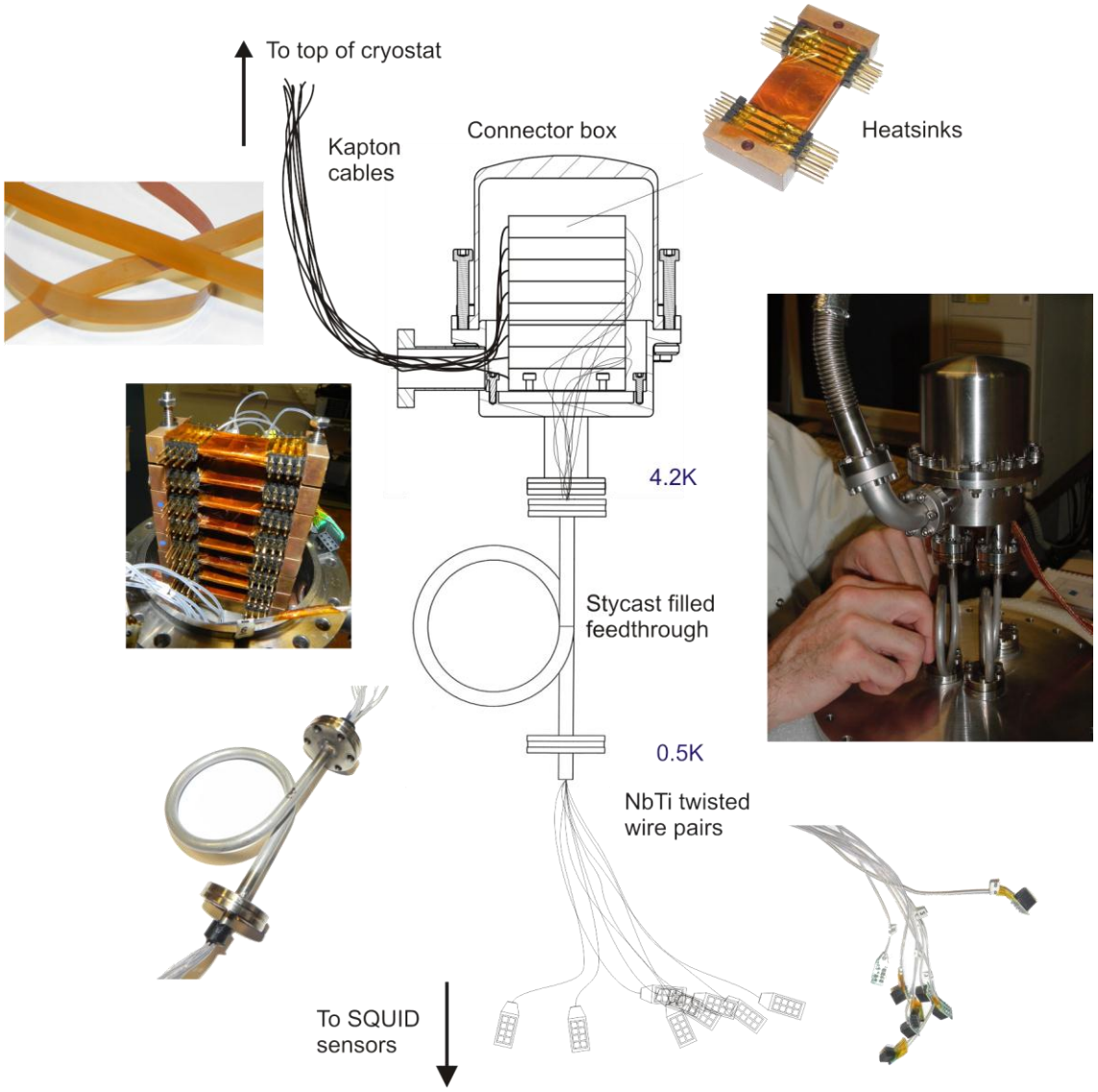

Figure 11 A schematic drawing showing the 4.2K connector box and Stycast filled tubes to join the Kapton cables from the top of the cryostat, to the SQUID sensors inside the superfluid volume, with photographs of the main components.

Material	**Heat load [µW] 4.2K – 0.5K**
NbTi wires	0.56
Stycast	9.2
Stainless steel tube walls	23
Total heat load 0.5K	32.8

Table 2 Heat load through the Stycast filled feedthroughs between the 4.2K connector box and the superfluid volume. The thermal conductivities used for these calculations were taken from [47-49].

The heat load through the Stycast filled tubes from the 4.2K level to the superfluid, given in Table 2 is dominated by the stainless steel walls of the tubes and the Stycast. To minimise this, the

feedthroughs are bent into a spiral shape to increase the total length, while allowing it to fit in the restricted space inside the cryostat. The contribution due to the superconducting wire is not significant.

The twelve SQUIDs each require four twisted wire pairs to carry the signals for the bias and modulation/feedback current, the voltage measurement and the heater connection. The design also includes sixteen wire pairs to carry signals to the loop heaters (see section 6.4), the calibration coils (6.3), and the compensation coil. Filters are installed on the heater and calibration coil lines in the 4.2K and top connector boxes.

The Stycast filled feedthroughs were manufactured as follows. First a set of 64 ~1m lengths of NbTi wires (0.125mm diameter) were twisted together into sets of four pairs, and pulled through lengths of PTFE sleeving. The sleeving was designed to protect both ends of the wires outside of the feedthrough from damage. The central section inside the feedthrough was left bare to allow the Stycast to flow around the wires. The eight sets of four TWPs were fed through the stainless tube. The tube was filled with degassed Stycast FT2850 under vacuum so no air pockets were introduced. Once the bulk of the tube was filled, the two ends were capped as shown in Figure 12.

This feedthrough followed a standard design for low temperature vacuum feedthroughs [47], however as the width of the tube and the number of wires was much greater than usual it was not expected to be vacuum-tight at low temperatures. The tube from the 4.2K connector box to the top of the cryostat was designed to be filled with helium gas as it is isolated from the main vacuum. Nonetheless we found some of the tubes constructed were leak-tight at superfluid temperatures and we are now investigating the production process in more detail with the aim of learning how to reliably produce superfluid-tight feedthroughs for these larger numbers of wires.

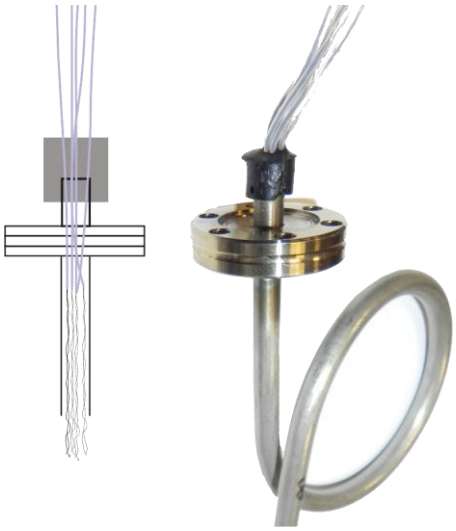

Figure 12 The end caps of the Stycast feedthroughs. The twisted wire pairs are protected by PTFE sleeving. The Stycast cap covered the edges of the stainless-steel tube protruding through a CF flange.

Mechanical damage to the wires was a serious issue for early prototypes. To make the feedthrough as robust as possible and prevent damage to the wires during installation, it was important to prevent Stycast creeping up the inside of the PTFE sleeving. This was done by selecting the smallest possible diameter of sleeving and sealing the ends with a small amount of vacuum grease. To test the durability of these feedthroughs, weights were attached to the wires and allowed to swing back and forth for ten minutes. The feedthrough was then checked for broken wires, and the weight was then progressively increased until the first connections were broken. The final design did not suffer any damaged until a weight of 8N was applied – far greater than that anticipated during normal use.

The 4.2K connector box is a stainless steel container divided in two halves, joined by an indium seal. The Stycast filled feedthroughs, and the stainless steel tube, which carries the Kapton cables to the

top of the cryostat connect to the box through copper gaskets seals. The cables are terminated with Samtec connectors which plug onto heat sink or filter boxes made from copper on Kapton circuits, stuck to a solid copper base with Stycast, as shown in Figure 11. This is a design used for the readout for the CRESST dark matter search [43].

6.7. Kapton cables, connectors and filters at top of cryostat: 300K – 4.2K

The connections from 4.2K to the top of the cryostat are made by flat ribbon cables made from Kapton with stainless steel tracks. Single grounded 'shielding tracks' run between the pairs of tracks to reduce crosstalk. The stainless steel tracks have low thermal conductivity.

The heat load estimate from room temperature to the 4.2K connector box is given in Table 3. The total heat load from the Kapton cables running from room temperature to 4.2K is 5.2mW. The stainless steel walls of the tube carrying the cables have a much greater area than the tracks, but they can be thermally anchored to the liquid nitrogen shield at an intermediate point reducing the heat load. This is still greater than that from the cables. This heat load is absorbed by the liquid helium bath to which the connector box is thermally coupled with a copper braid.

Table 3 also gives the heat load which would have been introduced by 32 copper wires. This design option was used in an early prototype (using woven cables as designed for the CRESST SQUID readout [43]) as using low resistance copper wires to measure the voltage across the SQUID is known to reduce the noise and increase the slew rate. However this improvement was marginal, and was not a limiting factor in the cryoEDM system, therefore the final version used stainless steel tracks on Kapton cables.

At the top of the cryostat, the Kapton cables plug onto circuit boards, connected to a flange-mounted 64-way SCSI connector. Three such connectors are fixed onto three KF-50 flanges on a cross-piece as shown in Figure 13. Two each carry the readout for six SQUID channels, the third, used for the signals for the calibration coils and heaters, has a set of filters mounted behind the SCSI filter to block high frequency electromagnetic noise.

Temperature drop	**Material**	**Heat load [mW]**
300K – 4.2K	Stainless steel tracks	3.1
	Kapton cable	2.1
	(Copper wires)	(37)
77K – 4.2K	Stainless steel tube walls	8.2
	Total heat load on 4.2K	13.4

Table 3 Heat load introduced into the cryoEDM apparatus due to the SQUID system readout. The heat load from the Kapton cables is much less than the stainless steel tube containing the cables (this can be thermally anchored at an intermediate 77K level, reducing the heat load on the 4.2K level). Also shown is the heat load from alternative cabling using copper wires for the SQUID voltage measurement. Due to the intermediate 4.2K level the heat load onto the superfluid is not significant. The thermal conductivities used for these calculations were taken from [47-50].

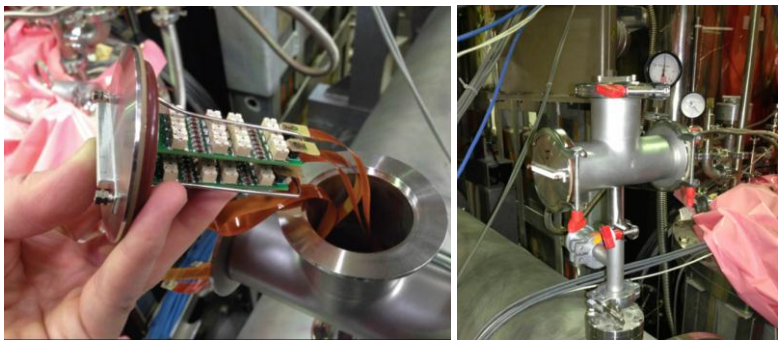

Figure 13 Left: Filter boards mounted behind a SCSI connector on a flange on the top of the cryostat. Right: Three flanges are mounted on a T-piece.

Figure 14 Clockwise from top right: The SQUID control and digitisation electronics; mounted on the cryostat; the USB modem; with power supply and control laptop.

6.8. Readout electronics and software

The control and digitisation electronics is mounted on top of the cryostat next to the connectors as shown in Figure 14. This consists of two STAR Cryoelectronics PFL800 preamplifier units, attached to custom-made units to control the system. These units handle the communication with the PFL800, generate a test signal to calibrate the SQUIDs, and digitise the output signal.

These units are connected to a PC by an optical fibre link and a USB modem. This minimises electromagnetic compatibility issues. The system can be controlled using a laptop computer through the USB interface if necessary. A DAC unit, mounted with the SQUID electronics, generates the signals applied to the calibration coils and heaters. A separate ADC is used to measure current drawn by each channel.

A similar data acquisition system was used to digitise the signals from a number of fluxgate magnetometer sensors located inside and outside the cryostat. Both systems are run from the same PC using integrated software.

An extensive suite of data acquisition software has been developed in C++ and the ROOT framework. This allows continuous running of the system, and can be controlled remotely if necessary. During

routine running, the outputs of the twelve channels are recorded every 1ms. The raw data is written to file to allow subsequent analysis. The system is designed to operate independently, but to allow data streams to be passed to a separate data acquisition system to be recorded with neutron data. Figure 15 shows screenshots of the programs used to tune the SQUID sensors and monitor the data recording.

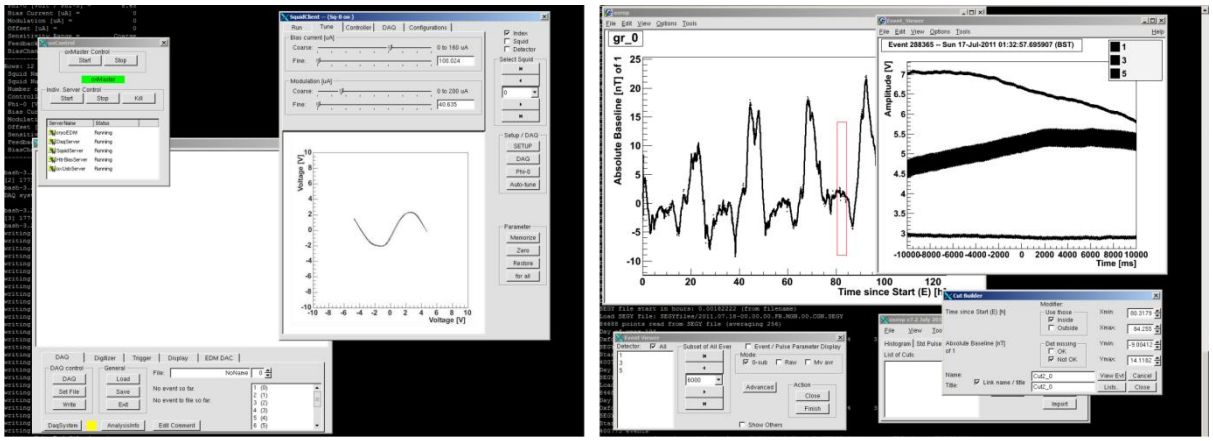

Figure 15 Screenshots from the software used to tune the SQUIDs and monitor the data acquisition (left), and for later data analysis (right).

7. Data processing

The data files written by the data acquisition program store the output of each SQUID channel (as a 16-bit number), typically sampled every 1ms. These files can be read using a specially written analysis program, written using the ROOT framework[3], in which the user can develop and run macros to perform specific analysis tasks. In addition the data acquisition software has the option to run a real time analysis to give an output value (a preliminary estimate of the magnetic field) which can be passed to another system running on a separate PC. An extensive set of programs and macros have been developed to perform expected analysis tasks. We expect these will be developed further when the data from a neutron EDM measurement is available.

The magnetometry data processing tasks include the following:

- **Remove reset/flux jump artefacts:** The timestamp for resets – when the output voltage approaches the ±10V limit and the feedback loop is momentarily opened to induce a flux jump to return the signal to ~0V – is logged by the data acquisition server. This log can be used to offset the SQUID signal to give a corrected magnetometry signal. Macros can also find and correct signal jumps above a given magnitude to deal with spontaneous flux jumps. This method works well in a suitable magnetic environment, as long as the external field does not change faster than the SQUID slew rate [36,53].
- **Remove crosstalk:** Crosstalk between pick-up loops occurs as the feedback current applied to a SQUID will change the current through its input loop which can be detected by a nearby loop. This can be corrected using software as described in [36]. This will only be significant if there are closely spaced parallel pick-up loops.
- **Calibration:** Given a calibration factor measured from tests using the calibration coils described in section 6.1, we can compute the signal for the average magnetic field through each loop.
- **Data quality monitoring:** It is important to identify periods of data where external interference or rapidly changing fields mean the flux jump correction is not possible. This is

[3] http://root.cern.ch/

assessed using parameters such as the number of resets over a given period; the maximum signal change (dV/dt); or the shortest time between two resets.

- **Extrapolation:** The analysis steps described so far produce a series of data sets giving the magnetic field at the position of each pick-up loop, in that direction. The next step is to use these data to extrapolate the magnitude of the average magnetic field across the neutron cell volume. This value will be 'calibrated' using the neutron precession frequency measured in zero electric field (to exclude any effect of an electric dipole moment, which we will then search for).

We propose to calculate our final magnetic field signal S_{NC} for each neutron cell, using a linear scaling as follows:

$$S_{NC}(t) = \sum_{i=1}^{12} \alpha_i S_i(t)$$

where S_i (t) are the twelve SQUID signals. The scaling parameters α_i will be calculated to minimise

$$\sum (S_{NC} - B_{NC})^2$$

where B_{NC} is the field in the neutron cell determined from the precession frequency. The summation is over all data points within a set calibration period over which significant field fluctuations were seen. Once the scaling parameters are calculated, they can be used to extrapolate the field in the neutron cell at future times.

The success or failure of this extrapolation will depend on the magnetic environment inside the apparatus. Numerical models of the magnetic field in which the field sources are magnetic dipole a long distant from experiment, show the technique works very well, as this gives a very uniform field in volume of the neutron cell and SQUID loops. The extrapolation does not work well for models with dipole sources close to the experiment (giving much larger gradients). Provided there are no significant time varying magnetic sources inside the main magnetic shield we are confident this method can reproduce the field inside the neutron cell as required for cryoEDM.

The decision to use twelve SQUID channels was taken during the design phase as a compromise between the need to allow an accurate extrapolation of a non-ideal field, and the need to keep the number of channels manageable.

Calculation of the scaling parameters can be done by matrix inversion, but if the SQUID data sets are highly correlated, it may be more effective to use a neural nets approach as described in [51,52]. A key benefit of this approach is that it does not require any model of the sources of magnetic field fluctuations. Once the coefficients are known, it can be calculated quickly, in real time if necessary. And it is flexible – if some SQUID channels are not available, then we can calculate coefficients for a system with a smaller number of parameters. The accuracy of this extrapolation will ultimately be limited by the field uniformity.

While a full demonstration of this technique must wait until it can be used in a neutron resonance measurement, we have tested this approach with data taken with a 3-axis system at the LSBB laboratory, as outlined in Section 8.

8. Magnetic field measurements at the low noise underground laboratory, Rustrel, France

The SQUID system has been installed in the cryoEDM apparatus, cooled to superfluid temperatures and used to monitor the magnetic field fluctuations over several periods of many weeks. It has not

yet been used as part of a neutron EDM measurement. However, the system has been used to characterise the magnetic environment and investigate sources of magnetic fields, such as the movement of magnetic materials around the apparatus. Preliminary SQUID data taken in these commissioning runs are presented in [53,54].

To assess the performance of our system we have conducted a series of tests at the Laboratoire Souterrain à Bas Bruit (LSBB), Rustrel France, away from the magnetic field disturbances due to other experiments, traffic and building activities. In this underground location the magnetic environment is limited only by geomagnetic fluctuations [55]. These tests were conducted with a compact version built to fit into a portable liquid helium dewar.

We tested an assembly of five SQUIDs with parallel pick-up loops. With this, we demonstrated a noise level (limited by geomagnetic fluctuations) of $4.0 fT Hz^{-1/2}$ above 1Hz and $(4.9/(f/1Hz))\ fT \cdot Hz^{-1/2}$.

We believe that in a suitable environment our system will meet its design specification to track magnetic field changes in the neutron cell to 0.1pT. However the intrinsic resolution of the system cannot be directly measured as even in the low noise environment at LSBB we were limited by the external magnetic fluctuations. As explained in section 4, the intrinsic SQUID noise (measured with a SQUID with the pick-up loop replaced by a short across the input) would give a resolution of 20fT. However this could, in principle, be impaired, for example if the system itself generates significant magnetic noise.

To test for this, we recorded data with two SQUIDs connected to the same pick-up loop. By taking the difference between the two signals we could subtract the magnetic signal and see the intrinsic SQUID noise spectrum. The resolution was then limited by the bit noise of the data acquisition, but there was no sign of low frequency magnetic noise which would impair performance. Full details of these tests are given in [36].

A plausible, if unlikely, concern is that the drift measured by our instrument may not be solely due to the external magnetic field. For example, if the flux-jump correction process introduces an erroneous shift.

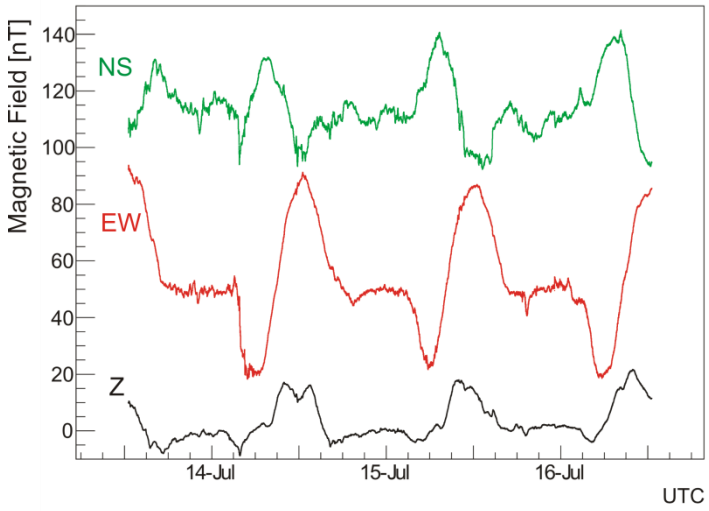

Figure 16 Magnetic field signals recorded using the cryoEDM SQUID system at the LSBB laboratory over a 72-hour period. These show the diurnal fluctuations due to ionospheric currents.

As a test of such effects, we carried out long period simultaneous measurements with a 3-axis version of the cryoEDM system, and the $[SQUID]^2$ magnetometer (SQUID in Shielding Qualified for Ionosphere Detection) [56] which is permanently installed at LSBB. These data, shown in Figure 16, allowed us to check the performance of our magnetometer against an independent SQUID system. This confirmed that both systems were tracking the same signal with an RMS difference over a 72-

hour period as low as 56pT [57]. This was limited by the gradient of the magnetic field between the two systems.

Thus we are confident that the system tracks the magnetic field as required. We have also used our system for a collaborative geophysics investigation into weak magnetic signals produced by groundwater flow.

This investigation also allowed us to check the extrapolation technique described in Section 7. We calculated the scaling coefficients to do a linear combination of the three channels recorded by our system, to fit a reference provided by the $[SQUID]^2$ magnetometer. In this case, the gradient of the magnetic field between the two systems was small, but the scaling allowed us to account for the misalignment of the two instruments and compare our signals accurately. The mathematics is the same but for a smaller number of channels. This analysis is outlined in [57].

9. Conclusions

In this paper we describe the instrument we have developed to monitor magnetic field fluctuations as part of a cryogenic neutron electric dipole moment experiment. This uses twelve SQUID sensors connected to pick-up loops close to the neutron cells. This is a novel approach for a neutron EDM experiment, designed to meet the requirement for 0.1pT precision magnetometry in a 0.5K superfluid helium environment.

We have outlined details of the components of this system and the results of tests carried out to ensure it meets these specifications without distorting the magnetic environment or introducing a significant heat load into the superfluid helium. We have installed the system in the cryoEDM apparatus at ILL, Grenoble, and demonstrated that it can be used to monitor magnetic fields. We have also run the system in the low noise environment at the Laboratoire Souterrain à Bas Bruit to demonstrate the performance which can be achieved in a suitable environment.

We have shown that our system will achieve a sub 0.1pT resolution if it is limited by the intrinsic SQUID noise. In practice the performance of any magnetometer is tied to the environment in which it will operate. However our tests at LSBB do not show reason why it should not achieve this.

This system meets the requirements for a cryogenic neutron EDM experiment. The performance in a neutron EDM measurement will be ultimately limited by the gradients of the magnetic signals across the neutron storage volume, which will limit the accuracy to which we can extrapolate the field in the neutron cell from measurements at points outside of this volume. To reach a sensitivity beyond that targeted by cryoEDM will most likely require a return to the co-magnetometer approach, necessitating the use of ^{3}He [15]. A system such as ours is a natural first step towards this, as SQUID sensors are the best way to measure the low frequency magnetic signal from precessing ^{3}He nuclei. An experiment could also use a hybrid approach using a combination of SQUID pick-up loops to track both the quasi-DC changes and the absolute magnitude (through the frequency of ^{3}He nuclei). We therefore anticipate this magnetometer design will be a useful reference for future EDM experiments.

Acknowledgements

This work was funded by STFC. We thank all our collaborators within the cryoEDM experiment, especially Maurits van der Grinten, Keith Green, Mike Pendlebury, Phil Harris and Mike Hardiman. The collaboration includes: the Universities of Oxford, Sussex, Swansea, Kure (Japan), the Rutherford Appleton Laboratory, and the Institut Laue-Langevin. We also thank Hans Kraus who designed the data acquisition hardware and software, and Michael McCann who wrote much of the software.

References

1. *Experimental searches for the neutron electric dipole moment,* SK Lamoreaux and R Golub, J. Phys. G: Nucl. Phys. 36 (2009) 104002. DOI: 10.1088/0954-3899/36/10/104002
2. *Improved Experimental Limit on the Electric Dipole Moment of the Neutron,* C. A. Baker et al., Phys. Rev. Lett. 97 (2006) 131801. DOI:10.1103/PhysRevLett.97.131801
3. *Performance of an atomic mercury magnetometer in the neutron EDM experiment*, K. Green et al., Nucl. Instrum. Meth. A 404, 381(1998). DOI: 10.1016/S0168-9002(97)01121-2
4. *Apparatus for measurement of the electric dipole moment of the neutron using a cohabiting atomic-mercury magnetometer,* C. A. Baker et al. Nucl. Instrum Meth. A 736 (2014) 184-203. DOI: 10.1016/j.nima.2013.10.005
5. *CryoEDM: a cryogenic experiment to measure the neutron Electric Dipole Moment*, C. A. Baker et al., International Conference on Neutron Scattering 2009, Journal of Physics Conference Series 251 012055. DOI:10.1088/1742-6596/251/1/012055
6. *CryoEDM: A cryogenic experiment to measure the neutron electric dipole moment,* M. van der Grinten, Nucl. Instrum. Meth. A 611, 129 (2009). DOI: 10.1016/j.nima.2009.07.040
7. *Measuring the electric dipole moment of the neutron: The cryoEDM experiment*, C. Clarke et al., Europhysics Conference on High Energy Physics. PoS(EPS-HEP 2009) 376. http://pos.sissa.it/archive/conferences/084/376/EPS-HEP%202009_376.pdf
8. *Plans for a Neutron EDM Experiment at SNS,* Takeyasu M Ito, J. Phys. Conf. Series 69 (2007) 012037. DOI: 10.1088/1742-6596/69/1/012037
9. *nEDM proposal to the Department of Energy,* http://p25ext.lanl.gov/edm/pdf.unprotected/EDM_proposal.pdf
10. *Experimental measurement of ultracold neutron production in superfluid ^{4}He,* C. A. Baker at al., Physics Letters A, 308 (2003) 67-74. DOI:10.1016/S0375-9601(02)01773-5
11. *Electric dipole moment searches: Effect of linear electric field frequency shifts induced in confined gases,* A.L. Barabanov, R. Golub and S.K. Lamoreaux, Phys. Rev. A 74 (2006) 052115.
12. *A Proposal for a Cryogenic Experiment to Measure the Neutron Electric Dipole Moment (nEDM),* S. N. Balashov et al., arXiv:0709.2428
13. *Experimental Limit to the Electric Dipole Moment of the Neutron,* J.H. Smith, E.M. Purcell and N.F. Ramsey, Phys. Rev. 108 (1957) 120-122. DOI:10.1103/PhysRev.108.120
14. *A search for the electric dipole moment of the neutron,* K.F. Smith et al., Phys. Lett. B 234 (1990) 191-196. DOI:10.1016/0370-2693(90)92027-G
15. *Development of a SQUID-Based He-3 Co-Magnetometer Readout for a Neutron Electric Dipole Moment Experiment*, Y. J. Kim and S. M. Clayton, IEEE Trans. Appl. Supercond. 23 (2013) 2500104, DOI: 10.1109/TASC.2012.2229773
16. *Detection of 3He spins with ultra-low field nuclear magnetic resonance employing SQUIDs for application to a neutron electric dipole moment experiment,* I Savukov et al., J. Mag. Res. 195 (2008) 129-133. DOI: 10.1016/j.jmr.2008.09.008
17. *Feasibility study of a ^{3}He-magnetometer for neutron electric dipole moment experiments,* Yu. Borisov et al. Nucl. Instrum. Meth. A 440 (2000) 483-488. DOI:10.1016/S0168-9002(99)01024-4
18. *New measurement of the neutron electric dipole moment,* A.P. Serebrov et al. JETP Lett. 99 (2014) 4-8.
19. *Search for the nEDM in vacuum and at ambient temperature.* http://nedm.web.psi.ch/EDM-world-wide/Neutrons/nEDM_PSI-Status_short.pdf
20. *Status of the nEDM measurement.* http://nedm.web.psi.ch/EDM-world-wide/Neutrons/nEDM_PSI-BVR_2012_Schmidt-Wellenburg.ppt

21. *Design and Performance of Laser-Pumped Cs-Magnetometers for the Planned UCN EDM Experiment at PSI,* S. Groeger et al. J. Res. Natl. Inst. Stand. Technol. 110 (2005) 179-183. DOI:10.6028/jres.110.021
22. *Quantum Magnetometer for stabilization of the neutron magnetic resonance,* EB Aleksandrov et al., Technical Physics letters, 32 (2006) 627-629. DOI: 10.1134/S1063785006070236
23. *A next generation measurement of the electric dipole moment of the neutron at the FRMII,* I. Altarev et al., Il Nuovo Cimento C 35, 122 (2012). DOI:10.1393/ncc/i2012-11271-0
24. *nEDM at KEK-RCNP the first step to nEDM at TRIUMF*, Y Masuda, http://fnp.kek.jp/English/workshop/nEDM_OakRidge2012/nEDM_KEK-RCNP.pdf
25. *Neutron electric dipole moment measurement with a buffer gas comagnetometer,* Y. Masuda et al. Physics Letters A 376 (2012) 1347-1351. DOI: 10.1016/j.physleta.2012.02.056
26. *An EDM measurement with a new comagnetometer and a high density UCN source,* K. Matsuta et al., 11th Conference on the Intersection of Particle and Nuclear Physics, AIP Conf. Proc. 1560, 152 (2013). DOI:10.1063/1.4826742
27. *A Molecular Beam Resonance Method with Separated Oscillatory Fields,* N.F. Ramsey. Phys. Rev. 78 (1950) 695-699. DOI:10.1103/PhysRev.78.695
28. *A New Source of Cold and Ultracold Neutrons,* A. Steyerl et al, Phys. Lett A 116 (1986) 347-352. DOI:10.1016/0375-9601(86)90587-6
29. *The interaction of Ultra-Cold Neutrons (UCN) with liquid helium and a superthermal UCN source*, R. Golub and J. Pendlebury, Phys. Lett. A 62 (1977) 337. DOI: 10.1016/0375-9601(77)90434-0
30. *Measurement of the ultra cold neutron production rate in an external liquid helium source,* P. Ageron et al., Phys. Lett. A 66 (1978) 469-471.
31. *Properties of cryogenic insulants,* J. Gerhold, Cryogenics 38 11 (1998) 1063-1081. DOI: 10.1016/S0011-2275(98)00094-0
32. *A new superleak to remove He^3 for UCN experiments,* H. Yoshiki, H. Nakai and E. Gutsmiedl, Cryogenics 45 (2005) 399-403. DOI: 10.1016/j.cryogenics.2005.01.007
33. *Development of solid state silicon detectors as ultra cold neutron detectors,* C. A. Baker et al., Nucl. Instr. Meth. A 487-3 (2002) 511-520. DOI: 10.1016/S0168-9002(02)00391-1
34. *Development of low temperature solid state silicon ultra cold neutron detectors working within superfluid ^4He,* C. A. Baker, Nucl. Instr. Meth. A 501-2 (2003) 517-523. DOI:10.1016/S0168-9002(03)00384-X
35. *The long-wavelength neutron spin-echo spectrometer IN15 at the Institut Laue-Langevin,* P. Schleger et al. Physica B 241 (1998) 164-165. DOI: 10.1016/S0921-4526(97)00539-5
36. *SQUID magnetometry for the cryoEDM experiment - Test at LSBB*, S Henry et al. JINST 3 (2008) P11003. DOI:10.1088/1748-0221/3/11/P11003
37. *The SQUID Handbook Vol. I Fundamentals and Technology of SQUIDs and SQUID systems,* Clarke J, Braginski A (2004), Wiley VCH.
38. *The SQUID Handbook Vol. II Applications of SQUIDs and SQUID Systems,* Clarke J, Braginski A (2004), Wiley VCH.
39. *First Results from a Superconductive Detector for Moving Magnetic Monopoles,* B. Cabrera, PRL 48 (1982) 1378. DOI:10.1103/PhysRevLett.48.1378
40. *Search for a flux of cosmic ray magnetic monopoles with an eight-channel superconducting detector,* M.E. Huber et al., Phys. Rev. D 44 (1991) 636. DOI: 10.1103/PhysRevD.44.636
41. *A direct search for stable magnetic monopoles produced in positron-proton collisions at HERA,* The H1 Collaboration, Eur. Phys. J. C 41 (2005) 133-141. DOI:10.1140/epjc/s2005-02201-6

42. *SuperCDMS Detector Readout Cryogenic Hardware,* D.N. Seitz et al., Low Temperature Detectors LTD 13, AIP Conf. Proc. 1185 (2009) 282-285. DOI:10.1063/1.3292334
43. *The 66-channel SQUID readout for CRESST II,* S Henry et al. JINST 2 (2007) P11003. DOI: 10.1088/1748-0221/2/11/P11003
44. *Design and performance of the ADMX SQUID –based microwave receiver,* SJ Asztalos et al. Nucl. Instrum. Meth. A 656 (2011) 39-44. DOI: 10.1016/j.nima.2011.07.019
45. *Development of superconducting contacts for the CRESST II 66-channel superconducting quantum interference device readout system,* B. Majorovits, S. Henry and H. Kraus, Rev. Sci. Instrum. 78 (2007) 073301. DOI: 10.1063/1.2754397
46. *Characterisation of superconducting capillaries for magnetic shielding of twisted-wire pairs in a neutron electric dipole moment experiment,* S Henry et al., accepted for publication in Nucl. Instrum. Meth. A .
47. *Matter and Methods at Low Temperatures, Frank Pobell. Springer-Verlag 1992.*
48. *Thermal conductivity of some common cryostat materials between 0.05 and 2 K, J. R. Olson. Cryogenics, 33, 729-731, (1993).* DOI: 10.1016/0011-2275(93)90027-L
49. *Experimental Techniques in Low-Temperature Physics, G. K. White, OUP 1979.*
50. *The thermal conductivity of Kapton HN between 0.5 and 5 K,* J. Lawrence, A.B. Patel and J.G. Brisson, Cryogenics, 40, 203-207 (2000). DOI: 10.1016/S0011-2275(00)00028-X
51. *Inflight magnetic characterization of the test masses onboard LISA Pathfinder,* M Diaz-Aguiló, E García-Berro and A Lobo, Phys. Rev. D 85 042004 (2012). DOI:10.1103/PhysRevD.85.042004
52. *Neural network interpolation of the magnetic field for the LISA Pathfinder Diagnostics Subsystem,* M Diaz-Aguiló, A Lobo, and E García-Berro, Exp. Astron. 30 1-21 (2011). DOI:10.1007/s10686-011-9215-8
53. *Magnetometry for cryoEDM.* Michael McCann. D.Phil thesis, University of Oxford (2012). http://ora.ox.ac.uk/objects/uuid:0a503382-d356-4fd6-b877-65bd00df331b
54. *CryoEDM - The search for the electric dipole moment of the neutron, Christine Clarke. Seminar, SLAC, 19 April 2011.* http://www.slac.stanford.edu/exp/seminar/talks/2011/20110419_Clarke.pdf
55. *The low noise underground laboratory of Rustrel-Pays d'Apt,* G. Wayand, J. Phys Conf. Ser. 39: 157. DOI: 10.1088/1742-6596/39/1/037
56. *Seismo-ionosphere detection by underground SQUID in low-noise environment in LSBB-Rustrel, France,* G Waysand et al., Eur. Phys. J. Appl. Phys. 47 (2009) 12705. DOI: 10.1051/epjap:2008186
57. *Tracking geomagnetic fluctuations to picotesla accuracy using two superconducting quantum interference device vector magnetometers,* S Henry, E Pozzo di Borgo and A Cavaillou. Rev. Sci. Instrum. 84 (2013) 024501. DOI: 10.1063/1.4790715